Space Structure Control Design by Variance Assignment

Robert E. Skelton*
Purdue University, West Lafayette, Indiana
and
Michael DeLorenzo†
U.S. Air Force Academy, Colorado Springs, Colorado

The performance requirements of spacecraft missions are usually specified in terms of root-mean-squared (rms) values on both the input and output variables. The rms contribution of each input or output in the overall system performance metric is called the "input" or "output" cost. A technique is derived that allows a linear controller to *assign* each of the multi-input or output costs. The procedure is illustrated by the design and shape control for NASA's 64-m Hoop-Column Antenna subject to power-limited actuators. By assigning only the output costs rather than the input costs, the procedure serves to determine the power *required* of the actuators (required input costs) to achieve the mission requirements (specified output costs). This determination of actuator sizing (and location) for the control of flexible structures is an important feature of the method.

I. Introduction

THE problem of regulating linear systems which have some form of amplitude constraints on either the system inputs or outputs has a wide range of practical engineering applications. The authors are motivated specifically by large space structures where the inputs represent noisy actuator signals, and the outputs represent line-of-sight pointing errors, deflections from a desired shape, etc. These structures have mission requirements naturally stated in terms of variance constraints on the outputs, subject to variance constraints on the actuator inputs (such as power limitations).

Referred to by NASA as the "hoop-column" antenna, the antenna configuration in Fig. 1 is one candidate under study for a large communications satellite to be positioned in geosynchronous orbit. Several (four are shown) transmitter/receiver units are positioned at the focal point (node 10 in Fig. 1) of the 64-m dish. The purpose of the control system is to prevent excessive radio beam degradations at the Earth receivers. In turn, this requires that the thin membrane-like mesh antenna dish be maintained in an almost parabolic shape and that the radiometric centroid of the beam be pointed to the correct location. This pointing and focusing problem translates into mean-squared constraints on the 24 output variables listed in Table 1. The physical locations of these outputs are at certain nodal points of the finite element model. These points are depicted in Fig. 1 by node numbers 2, 6, 9, 10, 101, 107, 113, and 119. For all angles (outputs 1-6) the variance constraint is 22.8 arc-sec

$$\mathcal{E}_\infty y_i^2 \le \sigma_i^2, \quad \sigma_i = 22.8 \text{ arc-sec}, \qquad i = 1 \to 6 \tag{1a}$$

where $\mathcal{E}_\infty \triangleq \lim_{t\to\infty} \mathcal{E}$, and $\mathcal{E}$ is the expectation operator. For linear displacements the variance constraint is 0.158 mm.

$$\mathcal{E}_\infty y_i^2 \le \sigma_i^2, \quad \sigma_i = 0.158 \text{ mm}, \qquad i = 7 \to 24 \tag{1b}$$

The small torque devices are capable of mean-squared torques up to 100 (dyne-cm)^2.

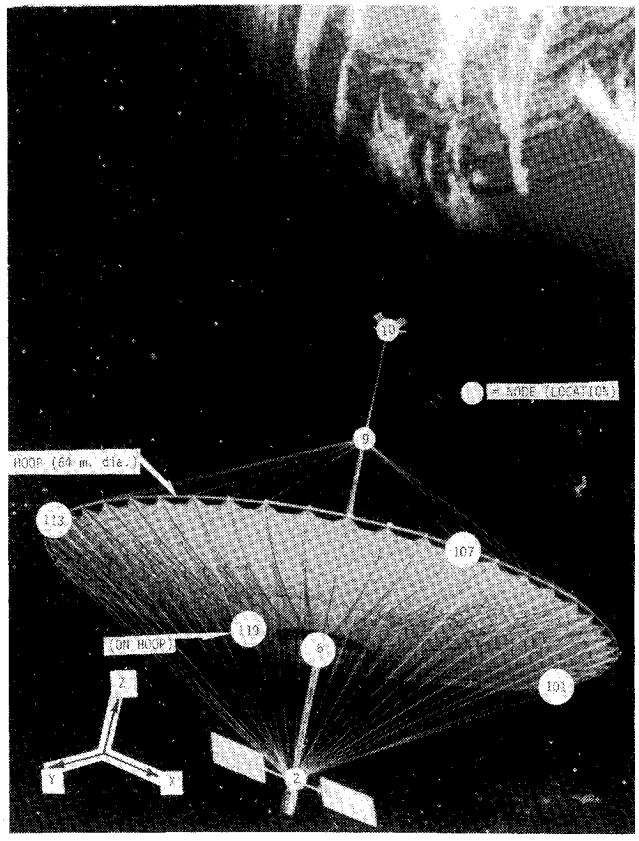

Fig. 1 Hoop-column antenna.

Table 1 Hoop-column output description

y_1 = AX2	y_9 = X9-X2	y_{17} = Y107-Y10
y_2 = AY2	y_{10} = Y9-Y2	y_{18} = Z107-Z10
y_3 = AZ2	y_{11} = X10-X2	y_{19} = X113-X10
y_4 = AX10-AX2	y_{12} = Y10-Y2	y_{20} = Y113-Y10
y_5 = AY10-AY2	y_{13} = X101-X10	y_{21} = Z113-Z10
y_6 = AX10	y_{14} = Y101-Y10	y_{22} = X119-X10
y_7 = X6-X2	y_{15} = Z101-Z10	y_{23} = Y119-Y10
y_8 = Y6-Y2	y_{16} = X107-X10	y_{24} = Z119-Z10

Submitted May 30, 1984, revision submitted Aug. 23, 1984.

*Professor, School of Aeronautics and Astronautics. Member AIAA.
†Captain. Member AIAA.

$$\mathcal{E}_\infty u_i^2 \le \mu_i^2, \quad \mu_i = 10 \text{ dyne-cm}, \qquad i = 1 \to 12 \tag{1c}$$

The 12 torquers producing torques u_i, $i = 1 \to 12$, are located as in Table 2, and the 39 sensors are located as in Table 3, where ARX2 means angular rate about the X axis at node 2, AX2 means angular displacement (inertially referenced) about the x axis at node 2, Z10-Z2 means rectilinear displacement between nodes 10 and 2 in the Z direction, etc. The actuator noise is described by zero-mean white noise with intensity

$$W = \text{diag}[\ldots W_{ii} \ldots], \quad W_{ii} = 0.1 \text{ (dyne-cm)}^2, \quad i = 1 \to 12 \tag{2}$$

The sensor noise is zero mean with intensity

$$V = \text{diag}[\ldots V_{ii} \ldots] \tag{3a}$$

where

$$V_{ii} = 7.61 \times 10^{-7} \text{ rad}^2 \qquad i = 1,2,3,13,14,15 \tag{3b}$$

$$V_{ii} = 2.50 \times 10^{-7} \text{m}^2 \qquad i = 4 \to 12, 16 \to 27 \tag{3c}$$

$$V_{ii} = 4.76 \times 10^{-5} \text{(rad/s)}^2, \qquad i = 28 \to 39 \tag{3d}$$

To illustrate the concepts in this paper, the dynamics of the antenna are described by the first ten elastic modes plus three rigid-body modes. The square of the modal frequencies in $(\text{rad/s})^2$ are

$$(\omega_1^2, \ldots, \omega_{13}^2) = (0, 0, 0, 0.406, 7.209, 7.236, 13.277, 44.834, 132.140, 142.660, 445.010, 448.690, 775.860) \tag{4}$$

The damping ratio assumed for all elastic modes is $\zeta_i = 0.005$, $i = 4 \to 10$. The mode shapes and mode slopes at the sensor, actuator, and output locations may be found in Ref. 2, and are described mathematically by $\{m_i, n_i\}$ $\mathcal{B}_i$, and (ρ_i, τ_i) respectively, as follows:

$$\ddot{\eta}_i + 2\zeta_i \omega_i \dot{\eta}_i + \omega_i^2 \eta_i = \mathcal{B}_i^T (u + w), \qquad i = 1 \to 13$$

$$y = \sum_{i=1}^{13} (\rho_i \eta_i + \tau_i \dot{\eta}_i), \quad z = \sum_{i=1}^{13} (m_i \eta_i + n_i \dot{\eta}_i) \tag{5}$$

where $\mathcal{B}_i \in R^{12}$, $y \in R^{24}$, $z \in R^{39}$ and z is the vector of measurements described in Table 3. The first control task is to regulate the antenna structure so that the outputs we wish to control, y_i, and the inputs, $\mathcal{U}_i$, satisfy

$$\mathcal{E}_\infty y_i^2 \le \sigma_i^2 \qquad i = 1 \to 24 \tag{6a}$$

$$\mathcal{E}_\infty u_i^2 \le \mu_i^2 \qquad i = 1 \to 12 \tag{6b}$$

The second objective is to select the critical sensors and actuators from the admissible set described in Tables 2 and 3, and to control the system with the reduced configuration of only 6 actuators and 12 sensors. The tools of input/output cost analysis[1] are used for both tasks, and the details of these notions will be described in Sec. II. The contribution that a state of the system makes in the overall quadratic performance metric is referred to as the "component cost," and this type of analysis was developed in Refs. 3-5. However, the idea of this paper is somewhat different. Instead of computing the cost of each *state* component we wish to compute the cost of each *input* and *output*, and not only to compute them but also to design the control system so that they take on specific values.

The paper is organized as follows. Section II presents a mathematical statement of the input/output variance assignment problem motivated by Eq. (6). Section III solves the variance assignment problem for a class of problems for which the Riccati equation has an analytical solution. Section IV presents an iterative algorithm to solve the more general variance assignment problem. Section V presents a mathematical statement of the input/output cost analysis problem which selects the critical actuators and sizes them to accomplish the required output performance [Eq. (6a)]. Section VI presents numerical results for NASA's 64-m Hoop-Column Antenna, using the *combined* sensor/actuator selection and variance assignment algorithms.

Table 2 Hoop-column actuatores, admissible set

Actuator	Torque	About axis	Node location
u_1	T	X	2
u_2	T	Y	2
u_3	T	Z	2
u_4	T	X	6
u_5	T	Y	6
u_6	T	Z	6
u_7	T	X	9
u_8	T	Y	9
u_9	T	Z	9
u_{10}	T	X	10
u_{11}	T	Y	10
u_{12}	T	Z	10

II. Input/Output Variance Assignment

Consider the system performance metric

$$\mathcal{V} = \mathcal{E}_\infty (\|y\|_Q^2 + \|u\|_R^2) \tag{7}$$

Table 3 Hoop-column sensors, admissible set

Sensor no.	Label	Sensor no.	Label	Sensor no.	Label
z_1	AX2	z_{14}	AY10	z_{27}	Z119-Z10
z_2	AY2	z_{15}	AZ10	z_{28}	ARX2
z_3	AZ2	z_{16}	X101-X10	z_{29}	ARY2
z_4	X6-X2	z_{17}	Y101-Y10	z_{30}	ARZ2
z_5	Y6-Y2	z_{18}	Z101-Z10	z_{31}	ARX6
z_6	Z6-Z2	z_{19}	X107-X10	z_{32}	ARY6
z_7	X9-X2	z_{20}	Y107-Y10	z_{33}	ARZ6
z_8	Y9-Y2	z_{21}	Z107-Z10	z_{34}	ARX9
z_9	Z9-Z2	z_{22}	X113-X10	z_{35}	ARY9
z_{10}	X10-X2	z_{23}	Y113-Y10	z_{36}	ARZ9
z_{11}	Y10-Y2	z_{24}	Z113-Z10	z_{37}	ARX10
z_{12}	Z10-Z2	z_{25}	X119-X10	z_{38}	ARY10
z_{13}	AX10	z_{26}	Y119-Y10	z_{39}	ARZ10

The closed-loop system which minimizes $\mathcal{V}$ is described by

$$\dot{x}=Ax+B(u+w) \qquad w\in R^{n_w}$$

$$y=Cx \qquad y\in R^{n_y}$$

$$z=Mx+v \qquad v\in R^{n_v} \tag{8}$$

$$\dot{\hat{x}}=A\hat{x}+Bu+F(z-M\hat{x})$$

$$u=G\hat{x} \qquad u\in R^{n_u} \tag{9}$$

By input and output cost analysis,[1] a decomposition of the total system performance metric gives these input costs,

$$\mathcal{V}_i^w = W_{ii}\|b_i\|^2_{K+L}, \qquad i=1,\ldots,m \tag{10a}$$

$$\mathcal{V}_i^v = V_{ii}\|f_i\|^2_L \tag{10b}$$

and these output costs

$$\mathcal{V}_i^y = q_i\|c_i\|^2_{P+\hat{x}}, \qquad q_i \triangleq Q_{ii} \tag{10c}$$

$$\mathcal{V}_i^u = r_i\|g_i\|^2_{\hat{x}}, \qquad r_i \triangleq R_{ii} \tag{10d}$$

where $\|\cdot\|^2_Q = (\cdot)^T Q(\cdot)$ and W, V, Q, R are assumed diagonal matrices, and where $K, L, P, \hat{X}, G, F$ satisfy

$$O=KA+A^TK-KBR^{-1}B^TK+C^TQC,$$

$$[g_1,\ldots,g_{n_u}]=G^T=KBR^{-1} \tag{11}$$

$$O=PA^T+AP-PM^TV^{-1}MP+BWB^T,$$

$$[f_1,\ldots,f_{n_z}]=F=PM^TV^{-1} \tag{12}$$

$$O=\hat{X}(A+BG)^T+(A+BG)\hat{X}+FVF^T \tag{13}$$

$$O=L(A-FM)+(A-FM)^TL+G^TRG \tag{14}$$

and $w(t)$, $v(t)$ are zero-mean uncorrelated white noises with intensities W, V, respectively. The input and output costs [Eqs. (10)] satisfy the cost decomposition property[1]

$$\mathcal{V}=\sum_{i=1}^{n_u}\mathcal{V}_i^u+\sum_{i=1}^{n_y}\mathcal{V}_i^y=\sum_{i=1}^{n_w}\mathcal{V}_i^w+\sum_{i=1}^{n_v}\mathcal{V}_i^v \tag{15}$$

Under our assumption of diagonal Q,R, the input/output costs are related to the input/output variances by

$$\mathcal{V}_i^u = q_i\mathcal{E}_\infty u_i^2 \tag{16a}$$

$$\mathcal{V}_i^y = r_i\mathcal{E}_\infty y_i^2 \tag{16b}$$

It is known[1] that $\{\mathcal{V}_i^w>0$ and $\mathcal{V}_i^v\geq 0\}$ if (A,C) and (A,M) are both observable pairs and (A,B) is controllable. If in addition, $(A-FM,G)$ is an observable pair, then $\mathcal{V}_i^v>0$. This latter event is not assured even if the *plant* controllability/observability conditions hold, since the optimal controller may still be nonminimal.[6] It is also known[1] that $\{\mathcal{V}_i^y>0$ and $\mathcal{V}_i^u>0\}$ if (A,C) and (A,M) are both observable pairs and (A,B) is controllable. If, in addition, $(A+BG,F)$ is a controllable pair, then $\mathcal{V}_i^u>0$. Furthermore, the closed-loop input/output costs $\mathcal{V}_i^v$, $\mathcal{V}_i^w$, $\mathcal{V}_i^y$, $\mathcal{V}_i^u$ are all invariant under state transformation $x=Tx$, $|T|\neq 0$.[1]

It is clear from Eqs. (16) that the problem of assigning a value to $\mathcal{V}_i^u$ or $\mathcal{V}_i^y$ is equivalent to assigning a value to $\mathcal{E}_\infty u_i^2$ or $\mathcal{E}_\infty y_i^2$, since $\mathcal{E}_\infty u_i^2=\mathcal{V}_i^u/q_i$ and $\mathcal{E}_\infty y_i^2=\mathcal{V}_i^y/r_i$. Hence, our problem of input/output cost assignment can and should be interpreted as an assignment of input/output *variances*. The input/output variances assignment problem will be solved by choosing weights q_i and r_i, if they exist, such that

$$\mathcal{V}_i^u/r_i=\mathcal{E}_\infty u_i^2\leq\mu_i^2, \qquad i=1,\ldots,n_u \tag{17a}$$

$$\mathcal{V}_i^y/q_i=\mathcal{E}_\infty y_i^2\leq\sigma_i^2, \qquad i=1,\ldots,n_y \tag{17b}$$

where μ_i and σ_i are specified by the mission performance requirements. There are two options in the subsequent algorithm; to solve these two variations of the problem.

The Input-Variance Assignment (IVA) Problem

For the system [Eq. (8)], find q_i, r_i such that the constraints [(Eq. (17a)] are binding ($\mathcal{E}_\infty u_i^2=\mu_i^2$), and the constraints [(Eq. (17b)] are relaxed by the smallest amount

$$\left\{\min\sum_i(\mathcal{E}_\infty y_i^2-\sigma_i^2)\forall i\ni\mathcal{E}_\infty y_i^2>\sigma_i^2\right\}$$

The Output-Variance Assignment (OVA) Problem

For the system [Eq. (8)], find q_i,r_i such that the constraints [Eq. (17b)] are binding ($\mathcal{E}_\infty y_i^2=\sigma_i^2$), and the constraints [Eq. (17a)] are relaxed by the smallest amount:

$$\left\{\min\sum_i(\mathcal{E}_\infty u_i^2-\mu_i^2)\forall i\ni\mathcal{E}_\infty u_i^2>\mu_i^2\right\}$$

Much has been written on the subject of weight selection in linear quadratic Gaussian (LQG) problem, but most methods are concerned with pole assignment rather than input or output cost assignment.[7-9] Others[10-13] deal with the relationships between the weights and sensitivity. Sesak et al.[14,15] use weights to reduce the controllability of certain (truncated) states. Perhaps the first suggestion for weight selection to achieve variance constraints appears in Ref. 16, and this work is based on that paper and Ref. 2. However, earlier work treats hard constraints of input amplitude.[17-19] Adaptive control with these objectives in mind has also been investigated in Ref. 20.

It is also clear that our problem is related to a vector performance index problem,[21] since each required variance can be considered as an element in such a performance vector. However, we must not draw too close an analogy with that problem since we seek an assignment of variances restricted by the selection of weights in the standard LQG problem. This approach is chosen, as opposed to the nonlinear mathematical programming approach of Ref. 20, in order to yield a linear controller.

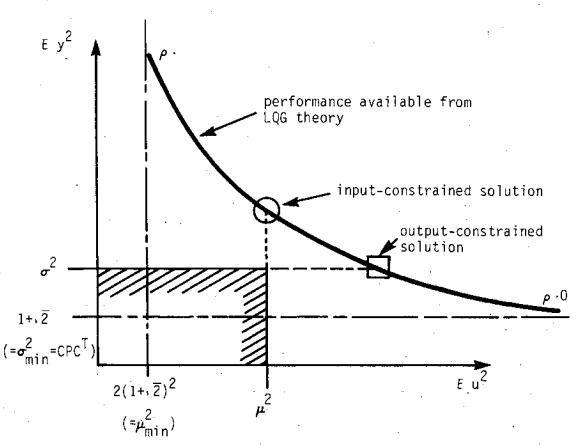

Fig. 2 Input/output cost assignment.

III. Special Problems with Analytical Solutions

For the case of the scalar plant with scalar input and output the cost assignment problem can be solved without the need of iterative algorithms. The purpose for showing such solutions is to illustrate the difficulties encountered in the multi-input/multi-output case.

For scalar y and u the cost function $\mathcal{V}$ can, without loss of generality, be written in the form

$$\mathcal{V} = \mathcal{E}_\infty (y^2 + \rho u^2)$$

where $\rho = Q^{-1}R$ is the single weight to be chosen so that the mean-squared performance lies within the shaded region of Fig. 2. For the example $\dot{x} = x + u + w$, $y = x$, $z = x + v$, the inequalities [Eqs. (17)] become

$$1 + \sqrt{2} + \frac{(1+\sqrt{2})^2}{2\sqrt{1+\rho^{-1}}} \le \sigma^2 \tag{18a}$$

$$\frac{(1+\sqrt{2})^2}{2\sqrt{1+\rho^{-1}}}(1+\sqrt{1+\rho^{-1}})^2 \le \mu^2 \tag{18b}$$

This leads to the conclusion that ρ must satisfy, from Eq. (18a)

$$\sqrt{1+\rho^{-1}} \ge \frac{(1+\sqrt{2})^2}{2(\sigma^2 - 1 - \sqrt{2})} \qquad \text{if } \sigma^2 > 1+\sqrt{2} \tag{19a}$$

$$\rho = 0 \qquad \text{if } \sigma^2 = 1+\sqrt{2} \tag{19b}$$

ρ has no solution of Eq. (18a) if $\sigma^2 < 1+\sqrt{2}$ (19c)

and from Eq. (18b),

$$\sqrt{1+\rho^{-1}} \le \frac{\mu^2}{(1+\sqrt{2})^2} - 1 + \sqrt{\left(\frac{\mu^2}{(1+\sqrt{2})^2} - 1\right)^2 - 1}$$

$$\text{if } \mu^2 \ge 2(1+\sqrt{2})^2 \tag{20a}$$

$$\rho = \infty \qquad \text{if } \mu^2 = 2(1+\sqrt{2})^2 \tag{20b}$$

ρ has no solution of Eq. (18b) if $\mu^2 < 2(1+\sqrt{2})^2$ (20c)

Clearly from these equations and Fig. 2, Eqs. (17) cannot be satisfied if

$$\sigma^2 < \sigma^2_{\min} = CPC^T = (1+\sqrt{2}) \tag{21}$$

or if

$$\mu^2 < \mu^2_{\min} = 2(1+\sqrt{2})^2 \tag{22}$$

Thus Eqs. (17) cannot be satisfied unless σ^2 and μ^2 are sufficiently large so that the solid curve from LQG theory intersects the shaded region of Fig. 2. In the absence of this circumstance two options will be available: "input-variance assignment" and "output-variance assignment." The input-variance assignment option seeks the solution $\odot$ along the dotted line in Fig. 2. That is, the input constraints [Eq. (11a)] are held binding, while the output constraints [Eq. (11b)] are relaxed by the smallest amount. The "output-constrained" option seeks the solution $\square$ along the dashed line in Fig. 2. That is, the output constraints [Eq. (11b)] are held binding, while the input constraints [Eq. (17a] are relaxed by the smallest amount. These ideas may be extended to the multi-input/multi-output case.

It is usually not possible to generalize the *explicit* inequalities [Eqs. (18)] for higher order systems, since closed-form solutions are not generally available for the Riccati equations.

IV. Weight Selection by Input/Output Cost Analysis: The Variance Assignment Algorithm

The following iterative algorithm is used to approximate the solution to the output variance assignment problem. (That is, Q, R will now be specified for a *given* sensor/actuator configuration.) As with most iterative algorithms, convergence proofs are not available. However, numerous numerical results are available and certain additional theoretical properties of the proposed algorithm are discussed in Ref. 2.

The Output-Variance Assignment (OVA) Algorithm

This algorithm is motivated by the output-variance assignment problem stated previously

$$\text{OVA:} \quad \min_{(Q,R)} \sum (\mathcal{E}_\infty u_i^2 - \mu_i^2) \forall i \ni \mathcal{E}_\infty u_i^2 > \mu_i^2$$

subject to

$$\mathcal{E}_\infty y_i^2 = \sigma_i^2 \qquad \forall i = 1 \to n_y$$

Step 1.

Specify $\{A, B, C, M, W, V, \sigma_i^2, \mu_i^2\}$

Compute

$$q_i(0) = \sigma_i^{-2}, \qquad i = 1 \to n_y$$

$$r_i(0) = \mu_i^{-2}, \qquad i = 1 \to n_u$$

Compute P. If for any i, $[CPC^T]_{ii} > \sigma_i^2$, stop. No solution exists which satisfies $\mathcal{E}_\infty y_i^2 \le \sigma_i^2$.

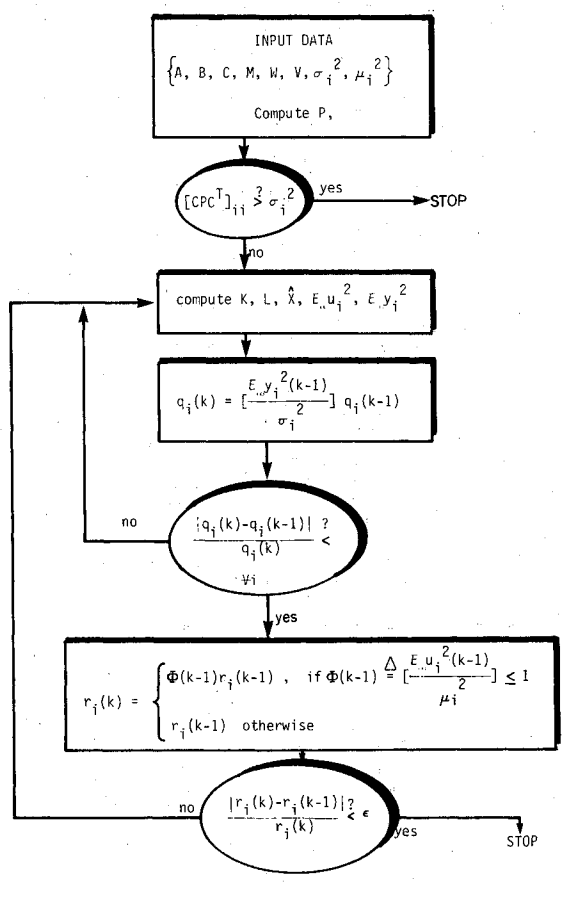

Fig. 3 OVA algorithm.

Table 4 Hoop-column antenna: output variance assignment

Iteration No. of the OVASAS algorithm	Deleted sensors (ν_i^{sen})		Deleted actuators (ν_i^{act})		Average input value	No. of sensors/ actuators
1	AZ10	(0.0004116)	TZ10	(−1.362)	3.275	39/12
	AZ2	(0.000397)	TZ9	(−1.369)		
	Z6-Z2	(0)				
	Z9-Z2	(0)				
	Z10-Z2	(0)				
2	AY10	(0.003362)	TZ6	(−2.1405)	3.592	34/10
	AX10	(0.003358)				
	AY2	(0.00226)				
	AX2	(0.00226)				
	Z113-Z10	(0.01942)				
	Z119-Z10	(0.001884)				
3	X6-X2	(0.01457)	TX10	(−1.2055)	3.699	28/9
	Y6-Y2	(0.01457)				
	Z101-Z10	(0.0110)				
	Z107-Z10	(0.0108)				
4	ARZ2	(0.02844)	TX9	(−1.21917)	3.997	24/8
	ARZ10	(0.02232)				
	ARZ6	(0.02238)				
5	X9-Z2	(0.0986)	TX6	(−1.4793)	4.377	21/7
	Y9-Y2	(0.0839)				
6	ARX6	(0.07648)		–	4.829	19/6
	ARX2	(0.07648)				
7	Y107-Y10	(0.13395)		–	4.857	17/6
	ARY9	(0.1098)				
8	X119-X10	(0.1557)		–	4.905	15/6
	X113-X10	(0.1555)				
	X101-X10	(0.1551)				
9		–		–	5.021	12/6

Step 2.
Compute $K, L, \hat{X}$, $\mathcal{V}_i^u/r_i = \mathcal{E}_\infty u_i^2$, $\mathcal{V}_i^y/q_i = \mathcal{E}_\infty y_i^2$.
Discussion: In the steady state,

$$\mathcal{V}_i^y(k) = \mathcal{V}_i^y(k-1)$$

where k is the iteration index. Hence,

$$q_i(k)\mathcal{E}_\infty y_i^2(k) = q_i(k-1)\mathcal{E}_\infty y_i^2(k-1)$$

and the iterations should stop when $\mathcal{E}_\infty y_i^2(k) = \sigma_i^2$. Hence,

$$q_i(k) = \left[\frac{\mathcal{E}_\infty y_i^2(k-1)}{\sigma_i^2}\right] q_i(k-1) \tag{23}$$

is used in the successive approximation. Repeat this process Eq. (23), continuing to update q_i until $\mathcal{E}_\infty y_i^2 = \sigma_i^2$, $i = 1 \to n_y$.

Step 3.
Similarly update r_i by

$$r_i(k) = \left[\frac{\mathcal{E}_\infty u_i^2(k-1)}{\mu_i^2}\right] r_i(k-1) \quad \text{if} \quad \left[\frac{\mathcal{E}_\infty u_i^2(k-1)}{\mu_i^2}\right] \le 1$$

$$= r_i(k-1) \qquad \text{otherwise} \tag{24}$$

Return to step 2 and continue this process until $q_i(k) = q_i(k-j)$ and $r_i(k) = r_i(k-j)$ for some j. When this occurs for $j = 1$ the algorithm has converged. When this occurs for $j > 1$ a limit cycle has been detected, and the algorithm stops. Small limit cycles will be acceptable (the final answer is "close" to a final solution). The authors have found that increasing the power of the bracketed terms in Eqs. (23) and (24) accelerates convergence.[2] No limit cycles have been

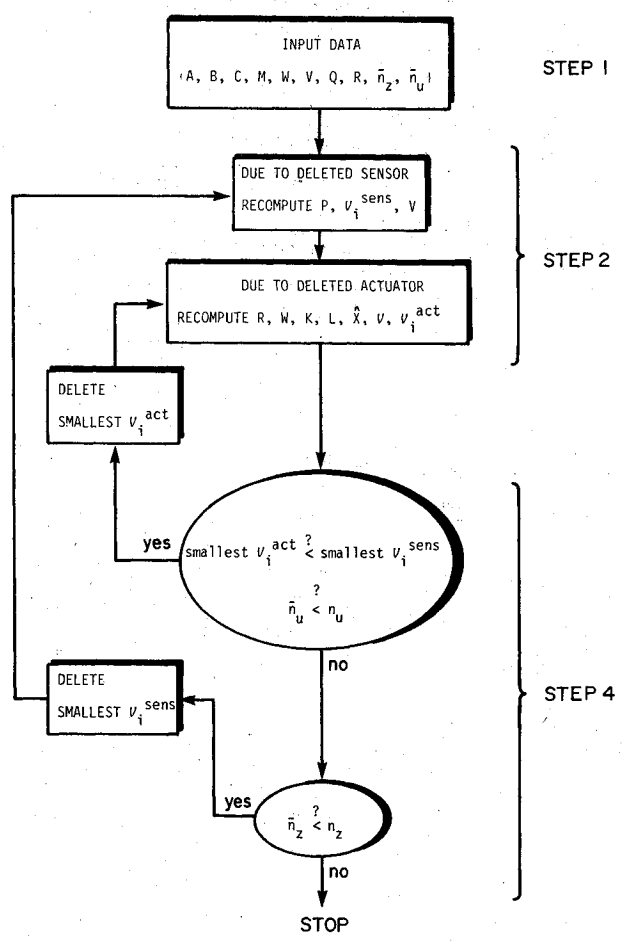

Fig. 4 SAS algorithm.

detected with this algorithm for a wide class of numerical examples with as many as 24 outputs and 12 inputs.

A flow chart of the OVA algorithm is given in Fig. 3. The input-variance assignment (IVA) algorithm is similar and will not be described separately.

If the OVA algorithm converges, it converges to a solution of the OVA problem stated previously. To see this, note that the algorithm takes

$$\mathcal{V} = \sum_{i=1}^{n_y} q_i \mathcal{E}_\infty y_i^2 + \sum_{i=1}^{n_u} r_i \mathcal{E}_\infty u_i^2 \tag{25}$$

to the value

$$\mathcal{V} = \sum_{i=1}^{n_y} q_{Mi}\sigma_i^2 + \sum_{i\notin\mathcal{I}} r_{Mi}\mu_i^2 + \sum_{i\in\mathcal{I}} \frac{\mathcal{E}_\infty u_i^2}{\mu_i^2} \tag{26}$$

where q_{Mi} is the steady value of q_i in Eq. (23) such that $\mathcal{E}_\infty y_i^2 = \sigma_i^2$; r_{Mi} is the final value of those r_i which were changed in Eq. (24) to achieve the equality on the right-hand side of Eq. (24); the remaining $r_i (i\in\mathcal{I})$ are not changed, $r_i = r_i(0) = \mu_i^{-2}$, yielding the last term in Eq. (26). Thus, subject to the constraints $\mathcal{E}_\infty y_j^2 = \sigma_u^2$, $\mathcal{E}_\infty u_i^2 = \mu_i^2$, $i\notin\mathcal{I}$ the minimization of

$$\sum_{i\in\mathcal{I}} \frac{\mathcal{E}_\infty u_i^2}{\mu_i^2} \forall i \ni \mathcal{E}_\infty u_i^2 > \mu_i^2$$

is accomplished by the minimum of Eq. (26).

The existence of q_{Mi} (such that $\mathcal{E}_\infty y_i^2 = \sigma_i^2$) is not guaranteed, but the existence of q_{Mi} such that $\mathcal{E}_\infty y_i^2 \le \sigma_i^2$ is guaranteed under the controllability assumptions. Thus, when the OVA algorithm [specifically Eq. (23)] finds $\mathcal{E}_\infty y_i^2 < \sigma_i^2$ it decreases q_i in an attempt to allow less control effort to permit $\mathcal{E}_\infty y_i^2$ to increase to its binding value $\mathcal{E}_\infty y_i^2 = \sigma_i^2$. But no matter how small one chooses q_i it may happen that $\mathcal{E}_\infty y_i^2$ does *not* increase. That is, in order to keep other outputs well behaved ($\mathcal{E}_\infty y_j^2 = \sigma_j^2$, $j \neq i$) it can happen that acceptable performance on y_i is "free" and need not be penalized in $\mathcal{V}$. In such cases the OVA algorithm will naturally drive such $q_i \to 0$ (we will observe this event in Table 6). Thus, when $q_{Mi} = 0$, the arguments of the above paragraph are still valid except for the technical footnote

$$\{q_{Mi} = 0 \text{ when } \mathcal{E}_\infty y_i^2 < \sigma_i^2, \text{ otherwise } \mathcal{E}_\infty y_i^2 = \sigma_i^2\}$$

The input variance assignment (IVA) algorithm is similar except for the opposite rules for updating q_i and r_i. Hence, the IVA algorithm which solves the IVA problem stated previously will not be written explicity.

V. Sensor/Actuator Selection by Input/Output Cost Analysis

It should be clear that the cost assignment problem is not independent from the problem of selecting sensor and actuator locations. This section treats the sensor/actuator selection problem as if Q, R were fixed.

Since $\mathcal{V}_i^u$ in Eqs. (10) represents the contribution of the ith input in the overall performance metric $\mathcal{V}$, and $\mathcal{V}_i^w$ represents the contribution of the noise from the ith actuator input, the "cost" of the ith actuator is measured by the difference between the "good" and "bad" effects.

$$\mathcal{V}_i^{act} = \mathcal{V}_i^u - \mathcal{V}_i^w \qquad \text{(actuator costs)} \tag{27}$$

and the "cost" of the ith sensor is measured by

$$\mathcal{V}_i^{sens} = \mathcal{V}_i^v \qquad \text{(sensor costs)} \tag{28}$$

The sensor signal z_i contains the sensor noise, $z_i = m_i^T x + v_i$, whereas the actuator signal u_i does not contain the noise w_i. Thus, each sensor and each actuator cost have different forms, [Eqs. (27) and (28)] but they are both linear combinations of input/output costs $\mathcal{V}_i^u$, $\mathcal{V}_j^w$, $\mathcal{V}_i^v$ obtained from the input/output cost analysis [Eqs. (10)]. Further support for Eqs. (27) and (28) is given in Refs. 1 and 2.

The magnitude of the Kalman filter gain on the ith sensor signal approaches zero as $V_{ii} \to \infty$,

$$\lim_{V_{ii}\to\infty} \|f_i\|^2 = \lim_{V_{ii}\to\infty} [m_i^T P P m_i / V_{ii}] = 0$$

(as does the sensor cost $\mathcal{V}_i^{sens} = \mathcal{V}_{ii}\|f_i\|_L^2 \to 0$). Hence, an extremely noisy sensor simply has no effect on the optimal LQG controller, yielding the result proved in Ref. 1.

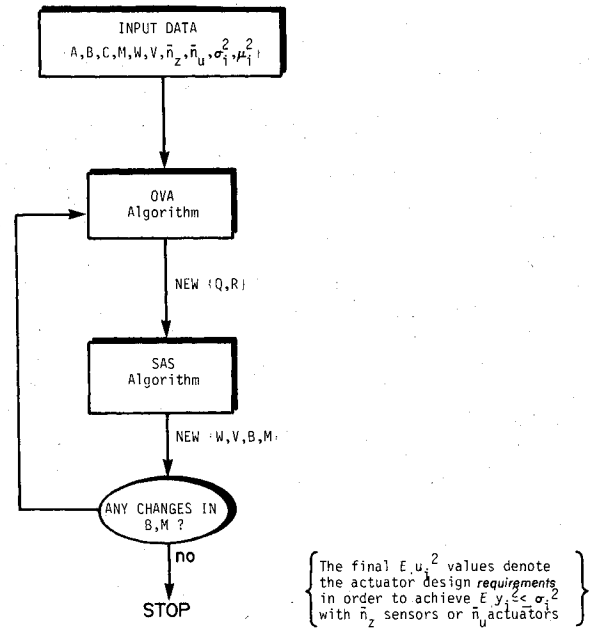

Fig. 5 OVASAS algorithm.

Table 5 Output variance assignment with six actuators

Outputs	$\sqrt{E_\infty y_i^2}$	Actuator no.	$\sqrt{E_\infty u_i^2}$, dyne-cm (design requirements)
y_1 = (AX2)	0.15 s	u_1 = TX2	72.91
y_2 = (AY2)	0.015 s	u_2 = TX2	26.145
y_3 = (AZ2)	11.588 s	u_3 = TZ2	105.47
y_4 = (AX10-AX2)	0.001 s	u_4 = TY6	26.138
y_5 = (AY10-AY2)	0.001 s	u_5 = TY9	31.750
y_6 = (AZ10)	12.000 s	u_6 = TY10	38.812
y_7 = (X6-X2)	0.010 mm		
y_8 = (Y6-Y2)	0.010 mm		
y_9 = (X9-X2)	0.068 mm		
y_{10} = (Y9-Y2)	0.068 mm		
y_{11} = (X10-X2)	0.158 mm		
y_{12} = (Y10-Y2)	0.158 mm		
y_{13} = (X101-X10)	0.104 mm		
y_{14} = (Y101-Y10)	0.158 mm		
y_{15} = (Z101-Z10)	0.007 mm		
y_{16} = (X107-X10)	0.158 mm		
y_{17} = (Y107-Y10)	0.156 mm		
y_{18} = (Z107-Z10)	0.008 mm		
y_{19} = (X113-X10)	0.122 mm		
y_{20} = (Y113-Y10)	0.158 mm		
y_{21} = (Z113-Z10)	0.001 mm		
y_{22} = (Z119-X10)	0.158 mm		
y_{23} = (Y119-Y0)	0.091 mm		
y_{24} = (Z119-Z10)	0.001 mm		

Theorem. For a given (Q,R) and a given set of sensors z_i, $i=1,\ldots,n_z$, the optimal value of the LQG performance metric $\mathcal{V}$ cannot be reduced by the deletion of any sensor z_i.

Thus, deleting sensors, (no matter how noisy they are), can never improve performance. This property does *not* carry over to the deletion of actuators. It may be possible to improve performance by deleting noisy actuators, as we shall show.

The $\mathcal{V}_i^{act}$ and $\mathcal{V}_i^{sens}$ represent the *in situ* contribution of an actuator and sensor and are only approximations to the amount by which the cost function is changed by the *deletion* of a sensor or actuator. That this approximation is quite accurate in practice is established in Refs. 1 and 2 by application to several large-scale systems. Based on input/output cost analysis, the proposed algorithm for selecting sensors and actuators from an admissible set is as follows.

The Sensor/Actuator Selection (SAS) Algorithm

Step 1.

Specify $\{A,B,C,M,W,V,Q,R,\bar{n}_z,\bar{n}_u\}$ where $\bar{n}_z \le n_z$ and $\bar{n}_u \le n_u$ represent the desired number of sensors and actuators to be used, and n_z,n_u represent the larger admissible set from which to choose.

Step 2.

Solve for $P,K,L,\hat{X}$ from Eqs. (1-14).

Step 3.

Compute $\mathcal{V}_i^{act}$ from Eqs. (10) and (23) and order according to

$$\mathcal{V}_1^{act} \ge \mathcal{V}_2^{act} \ge \mathcal{V}_3^{act} \ge \ldots \ge \mathcal{V}_{n_u}^{act}$$

Delete the actuator with the smallest algebraic value of $\mathcal{V}_i^{act}$ (that is, delete the ith column of B and the ith row and column of W and R). After each deletion recompute K, $\hat{X}$, L and again delete the smallest $\mathcal{V}_i^{act}$. Continue this iterative process until performance as measured by $\mathcal{V}$ from Eq. (15) ceases to improve [until $\mathcal{V}(k-1)$ th iteration) $\le \mathcal{V}(k$th iteration)]. Further deletion of *either* sensors or actuators will degrade performance.

Step 4.

Compute $\mathcal{V}_i^{act}$, $\mathcal{V}_i^{sens}$ and order the $\mathcal{V}_i^{act}$ and $\mathcal{V}_i^{sens}$ according to algebraic value,

$$\mathcal{V}_1^{sens} \ge \mathcal{V}_1^{act} \ge \ldots \ge \mathcal{V}_i^{act} \ge \mathcal{V}_j^{sens} \ge \ldots \text{etc.}$$

Delete the sensor or actuator device with the smallest algebraic value of $\mathcal{V}_i^{act}$, $\mathcal{V}_i^{sens}$ (to delete a sensor, delete the ith row of M and the ith row and column of V). Return to step 2 and repeat this process until either the remaining actuators are $\bar{n}_u$ in number, or the remaining sensors are $\bar{n}_z$ in number, whichever occurs first.

A flow chart of the SAS algorithm appears in Fig. 4. For simplicity in the diagram, Fig. 4 shows some unnecessary computation. Actually, when delecting sensors, K does not have to be recomputed. Step 3 is omitted from the diagram of Fig. 4 because it is not a necessary step. It should only be added if the analyst wishes to know the optimal actuator configuration with the full admissible set of sensors. In the NASA Hoop-Column Antenna example, six actuators were deleted in step 3 to improve performance prior to the deletion of any sensor. That is, the overall system gave better performance with 6 actuators than with the admissible 12. This is due to the contribution of more noise than signal from the six deleted actuators. [Note that this flaw in actuator selection *cannot* be detected a priori by simply looking at the noise data for each actuator. In our example *all* actuators had the same noise [Eq. (2)]. What makes some "too noisy" and others not, is the effect of location and control law.] Data for step 3 calculations may be found in Ref. 2 will not be included herein.

VI. Combined Sensor/Actuator Selection and Variance Assignment

Figure 5 shows the integration of the OVA and SAS algorithms and Table 4 shows the results for the hoop-column antenna with $\bar{n}_z = 12$, $\bar{n}_u = 16$. The average input value listed in Table 4 denotes

$$\frac{1}{n_u}\sum_{i=1}^{n_u} \mathcal{E}_\infty \frac{u_i^2}{\mu_i^2}$$

The total control effort (power),

$$\left[\frac{1}{n_u}\sum_{i=1}^{n_u} \mathcal{E}_\infty u_i^2\right] n_u$$

is $3.275 \times 12 = 39.30$ (dyne-cm)^2 which is about 25% *greater* than the control power needed to give the same output variance using 6 actuators, $5.021 \times 6 = 30.12$. Hence step 3 in the SAS algorithm deleted 6 actuators and better performance was obtained using *fewer* actuators, since the noise effect $\mathcal{V}_i^w$ was greater than the signal effect $\mathcal{V}_i^u$ (note the negative values of $\mathcal{V}_i^{act}$ in Table 4). Note also that all torquers about the Z axis (Fig. 1) have been deleted except one (TZ2). This is a logical result since the column is very rigid in torsional motion. Hence only one Z-axis torquer is required to maintain controllability.[22] It is interesting, however, that even one Z-axis torquer is required, since rigid antenna motion about the Z axis is unobservable in the pointing errors. The Z-axis torquer is actually retained because the *flexible* torsional motions seriously degrade antenna shape. The fact that none of the Y axis torquers were deleted suggests that the control of the motion fo the flexible solar array is important to the antenna performance. (See from Fig. 1 that solar array bending can produce torques about the Y axis.)

From column 2 of Table 4 the least important (deleted) sensors are listed. The fact that the sensors measuring "defocusing" deflections (Z6-Z2, Z9-Z2, Z10-Z2) had negligible sensor costs $\mathcal{V}_i^{sens}$ suggests that the antenna column is so stiff that these measurements are not important. As expected the Z-axis

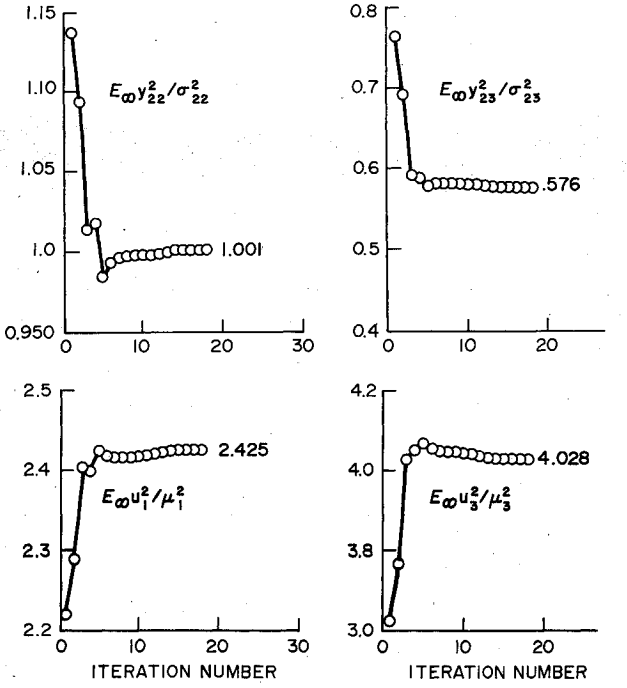

Fig. 6 Hoop-column antenna: output variance assignment (OVA) algorithm convergence.

Table 6 Hoop-column antenna: output variance assignment with 12 actuators

Outputs	$\sqrt{E_\infty y_i^2}$		Actuators[a]	$\sqrt{E_\infty u_i^2}$, dyne-cm (design requirements)
y_1	0.015 s	$(q_1=0)$	u_1=TX2	24.252
y_2	0.015 s	$(q_2=0)$	u_2=TY2	24.288
y_3	11.579 s	$(q_3=0)$	u_3=TZ2	40.280
y_4	0.001 s	$(q_4=0)$	u_4=TX6	24.253
y_5	0.001 s	$(q_5=0)$	u_5=TY6	24.282
y_6	12.001 s	$(q_6=0)$	u_6=TZ6	40.869
y_7	0.010 mm	$(q_7=0)$	u_7=TX9	29.466
y_8	0.010 mm	$(q_8=0)$	u_8=TY9	29.496
y_9	0.068 mm	$(q_9=0)$	u_9=TZ9	41.963
y_{10}	0.068 mm	$(q_{10}=0)$	u_{10}=TX10	36.026
y_{11}	0.158 mm		u_{11}=TY10	36.056
y_{12}	0.158 mm		u_{12}=TZ10	41.747
y_{13}	0.104 mm	$(q_{13}=0)$		
y_{14}	0.158 mm			
y_{15}	0.007 mm	$(q_{15}=0)$		
y_{16}	0.158 mm			
y_{17}	0.156 mm			
y_{18}	0.008 mm	$(q_{18}=0)$		
y_{19}	0.122 mm	$(q_{19}=0)$		
y_{20}	0.159 mm			
y_{21}	0.001 mm	$(q_{21}=0)$		
y_{22}	0.158 mm			
y_{23}	0.091 mm	$(q_{23}=0)$		
y_{24}	0.001 mm	$(q_{24}=0)$		

[a]Specification violation ($E_\infty u_i^2 > \mu_i^2$).

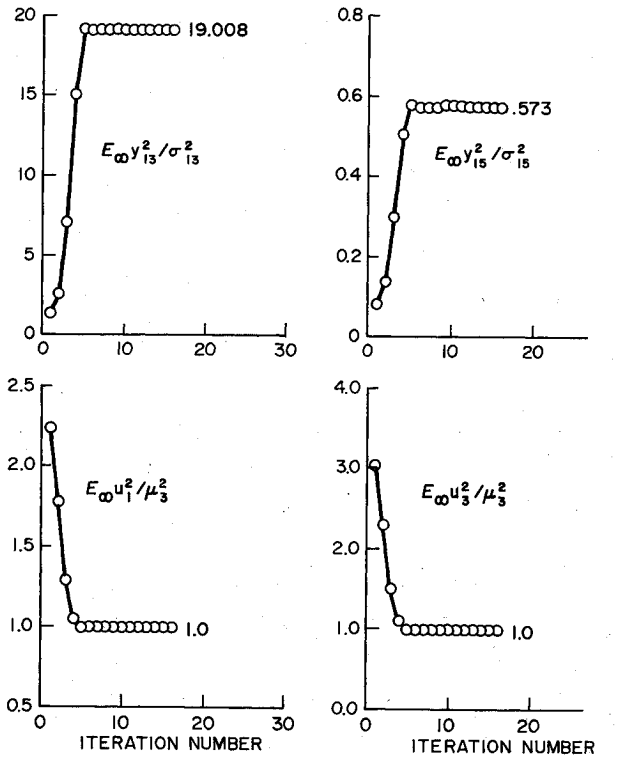

Fig. 7 Hoop-column antenna: input variance assignment (IVA) algorithm convergence.

attitude sensors AZ10, AZ2 are not important since the radio beam is not degraded by such motions. The 12 most important (retained) sensors are: X10-X2, Y10-Y2, Y101-Y10, X107-X10, Y113-Y10, Y119-Y10, ARY2, ARY6, ARY9, ARZ9, ARX10, ARY10. It is noted from this list that numerous rate gyroscope measurements (AR__) are quite important. Of the 12 admissible rate gyros, only three were deleted besides those mounted about the Z axis.

Table 5 describes the input/output variance performance of the final result (with 12 sensors and 6 actuators). Note that in this OVA problem all of the 24 outputs are at their assigned variances [Eq. (1)], except those that are less than their allowed variances, (outputs 1→10, 13, 15, 18, 19, 21, 23, 24). By using less control effort one might expect that these outputs could be increased to their allowed value. Such is not the case, because such action would permit other outputs to exceed their assigned variances. In fact, one of the striking conclusions of Table 5 is that very few system outputs have to be penalized to get the desired performance.‡ Every output which is less than its allowed value in Table 5 is associated with a zero weight $q_i \to 0$. This fact is made explicit in Table 6 which shows results using all 12 admissible actuators. Comparing Tables 5 and 6 yields the following conclusions. The output constraints [Eqs. (1a) and (1b)] are binding for only 7 of 24 outputs. The remaining outputs remain small (within their constraints) *regardless* of how small the weight q_i is made. That is, the 24 output variance constraints [Eqs. (1)], can be achieved by penalizing only 7 outputs in an LQG problem. These critical outputs are (X10-X2), (Y10-Y2), (Y101-Y10), (X107-X10), (Y107-Y10), (Y113-Y10), and (X119-X10). None of the critical outputs are angles, and yet the critical sensors were angle rates, see Table 4. This emphasizes the fact that it may be neither required nor even desirable to measure the same signals that are penalized. That is, to best control variable y it may be better to measure a *different* variable z (these conclusions disregard model error effects which are not considered in this paper). Furthermore, this output performance is essentially unaltered by the deletion of 6 actuators (compare the second column of Tables 5 and 6), and a saving of 25% control effort (compare the mean squared sum of the last column in Tables 5 and 6). Table 5 demonstrates the required *actuator design specifications*; actuator TZ2 should be designed for 105 dyne-cm torques. Actuator TX2 should be designed for 73 dyne-cm torques, etc. This information demonstrates the most important feature of the OVASAS algorithm: the determination of the design requirements for actuators of flexible structures. Sizing actuators for the control of *rigid* bodies is a relatively straightforward computation involving the disturbances. However, the sizing of actuators for the control of flexible structures has received little attention.

The results of Table 5 are obtained from the SAS and OVA iterative algorithms as combined in Fig. 5. The results of Table 6 are obtained from the OVA algorithm where the top half of Fig. 6 demonstrates the convergence properties of the OVA algorithm, which were typical for the 24 output variances, and the bottom half of Fig. 6 demonstrates the convergence properties which were typical for the 12 input variances. (The final values of all input and output variances appear in Table 6.)

Figure 7 demonstrates the typical convergence of the output and input variances of the IVA algorithm which yielded the results in Table 7 for the admissible set of actuators and sensors. These results determine the best performance that can be achieved with 12 actuators operating at their limits [the constraints, Eq. (1c), are binding]. In this case 14 of the 24 outputs exceed the requirements [Eqs (1a) and (1b)]. Hence, the mission objectives cannot be satisfied with 12 actuators with mean-squared output capabilities of 10 dyne-cm. In order to satisfy the mission requirements the actuators may be sized according to Table 5, obtained from the OVASAS algorithm.

It is important to note that the IVA problem (replacing the OVA algorithm in Fig. 5 by the IVA algorithm) will *not* generally yield the same sensor and actuator configurations as the OVA problem.[2] Indeed, it is important to consider the

‡This shows the frustration of trying to assign values to state weighting matrices in x^TQx terms commonly used in LQG problems. In this example, this would require the selection of 26 state weights, Q_{ii}, $i=1\to26$, when only seven are actively involved in achieving performance, even though all states are observable.

Table 7 Hoop-column input variance assignment

Outputs	$\sqrt{E_\infty y_i^2}$ (minimum achievable)		Actuators	$\sqrt{E_\infty u_i^2}$, dyne-cm
y_1 = (AX2)	0.171 s	($q_1 = 0$)	u_1 = TX2	10.000
y_2 = (AY2)	0.174 s	($q_2 = 0$)	u_2 = TY2	10.000
y_3^a = (AZ2)	701.807 s		u_3 = TZ2	10.000
y_4 = (AX10-AX2)	0.008 s	($q_4 = 0$)	u_4 = TX6	10.000
y_5 = (AY10-AY2)	0.008 s	($q_5 = 0$)	u_5 = TY6	10.000
y_6^a = (AZ10)	727.366 s		u_6 = TZ6	10.000
y_7 = (X6-X2)	0.122 mm	($q_7 = 0$)	u_7 = TX9	10.000
y_8 = (Y6-Y2)	0.120 mm	($q_8 = 0$)	u_8 = TY9	10.000
y_9^a = (X9-X2)	0.799 mm		u_9 = TZ9	10.000
y_{10}^a = (Y9-Y2)	0.784 mm		u_{10} = TX10	10.000
y_{11}^a = (X10-X2)	1.859 mm		u_{11} = TY10	10.000
y_{12}^a = (Y10-Y2)	1.824 mm		u_{12} = TZ10	10.000
y_{13}^a = (X101-X10)	3.003 mm			
y_{14}^a = (Y101-Y10)	7.595 mm			
y_{15} = (Z101-Z10)	0.091 mm	($q_{15} = 0$)		
y_{16}^a = (X107-X10)	7.218 mm			
y_{17}^a = (Y107-Y10)	3.381 mm			
y_{18} = (Z107-Z10)	0.090 mm	($q_{18} = 0$)		
y_{19}^a = (Y113-X10)	2.054 mm			
y_{20}^a = (Y113-Y10)	3.474 mm			
y_{21} = (Z113-Z10)	0.016 mm	($q_{21} = 0$)		
y_{22}^a = (Z119-X10)	3.728 mm			
y_{23}^a = (Y119-Y10)	1.799 mm			
y_{24} = (Z119-Z10)	0.010 mm	($q_{24} = 0$)		

[a]Constraint violation ($E_\infty y_i^2 > \sigma_i^2$).

specific control objectives in the selection of sensors and actuators. Controllability and observability studies[22,23,25,26] are not enough!

VII. Conclusions

This paper constructs iterative algorithms designed to assign specified mean-squared values to multiple inputs or multiple outputs. Input/output cost analysis is used to develop these algorithms which integrate the following tasks: The algorithms

1) Design a linear feedback controller which satisifes output variance constraints. This is accomplished by iterative weight selection in the LQG problem.

2) Select sensors and actuators from an admissible set of types and locations.

3) Determine actuator design requirements for the control of flexible structures to meet specified output variance constraints.

Numerical properties of the convergence of these algorithms are demonstrated for NASA's 64-m Hoop-Column Antenna.

To control the focus of a hoop-column-type antenna it is important to have three-axis torque control at the intersection of the flexible solar panel and the flexible antenna mast, and to have torque control along the mast about an axis perpendicular to the solar panel and the mast. One of these torquers should be located at the feed horns, near the focal point of the antenna. The required radio beam performance can be achieved using 12 sensors and 6 torque actuators with torque capabilities ranging from 26 to 105 dyne-cm.

Acknowledgments

The finite element model of the hoop-column antenna was computed by the Harris Corporation and provided by G. Rodriquez of the Jet Propulsion Laboratory. Portions of this work were sponsored by AFOSR Grant 82-0209 and NSF Grant ECS-8119598.

References

[1]Skelton, R.E. and DeLorenzo, M.L., "Selection of Noisy Actuators and Sensors in Linear Stochastic Systems," *Journal on Large Scale Systems, Theory and Applications,* Vol. 4, April 1983, pp. 109-136.

[2]DeLorenzo, M.L., "Selection of Noisy Sensors and Actuators for Regulation of Linear Systems," Ph.D. Thesis, School of Aeronautics and Astronautics, Purdue University, West Lafayette, Ind., May 1983.

[3]Skelton, R.E., "Control Design of Flexible Spacecraft," *Theory and Application of Optimal Control in Aerospace Systems,* edited by I.P. Kant, AGARDograph 251, June 1981, Chap. 8.

[4]Skelton, R.E. and Yousuff, A., "Component Cost Analysis of Large Scale Systems," *International Journal of Control,* Vol. 37, No. 2, 1983, pp. 285-304.

[5]Yousuff, A., and Skelton, R.E., "Controller Reduction by Component Cost Analysis," *IEEE Transactions on Automatic Control,* Vol. AC-29, June 1984, pp. 520-530.

[6]Yousuff, A. and Skelton, R., "A Note on Balanced Controller Reduction," *IEEE Transactions on Automatic Control,* Vol. AC-29, March 1984, pp. 254-257.

[7]Harvey, A.H. and Stein, G., "Quadratic Weights for Asymptotic Regulator Properties," IEEE Transactions on Automatic Control, Vol. AC-23, June 1978, pp. 378-387.

[8]Shaked, U., "The Asymptotic Behavior of the Root-Loci of Multivariable Optimal Regulators," *IEEE Transactions on Automatic Control,* Vol. AC-23, June 1978, pp. 425-429.

[9]Hartmann, Harvey, and Mueller, "Optimal Linear Control," Office of Naval Research, Arlington, Va., ONR CR215-238-1, Dec. 1975.

[10]Grimble, M.J. and Johnson, M.A., "Asymptotic Methods in the Selection of LQP Optimal Control Weighting Matrices," *IFAC Workshop on Singular Perturbations and Robustness of Control Systems,* Ohrid, Yugoslavia, July 1982.

[11]Athans, M., "The Role and Use of the Stochastic Linear-Quadratic Gaussian Problem in Control System Design," *IEEE Transactions on Automatic Control,* Vol. AC-16, Dec. 1971, pp. 529-551.

[12]McEwen, R.S. and Looze, D.P., "Quadratic Weight Adjustment for the Enhancement of Feedback Properties," *Proceedings of the 1982 American Control Conference,* Arlington, Va., June 1982, pp. 996-1001.

[13]Safonov, M.G., "Choice of Quadratic Cost and Noise Matrices and the Feedback Properties of Multiloop LQG Regulators," *Proceedings of 13th Asilomar Conference on Circuits, Systems, and Comp.,* Pacific Grove, Calif., Nov. 1979, pp. 203-205.

[14]Sesak, J.R., Likins, P., and Coradetti, T., "Flexible Spacecraft Control by Model Error Sensitivity Suppression," *Journal of Astronautical Sciences,* Vol. XXXVII, April-June 1979, pp. 131-156.

[15]Sesak, J.R. et al., "Constrained Optimal Compensation Design for Large Flexible Spacecraft Control," *Proceedings of the 19th IEEE Conference on Decision and Control,* Albuquerque, N. Mex., Dec. 1980, pp. 994-998.

[16]Skelton, R.E. and DeLorenzo, M.L., "On Selection of Weighting Matrices in the LQG Problem," *20th Annual Allerton Conference on Computing and Control,* Allerton, Ill., Oct. 1982, pp. 803-812.

[17]Goodwin, G.C., "Amplitude Constrained Minimum Variance Controller," *Electronic Letters,* Vol. 8, 1972, pp. 181-182.

[18]Toivonen, H., "Minimum Variance Control of First Order Systems with a Constraint on the Input Amplitude," *IEEE Transactions on Automatic Control,* Vol. AC-26, April 1981, pp. 556-558.

[19]Makila, P.M., Westerlund, T., and Toivonen, H.T., "Constrained Linear Quadratic Gaussian Control," *21st IEEE Conference on Decision and Control,* Orlando, Fla., Dec. 1982.

[20]Toivonen, H., "Variance-Constrained Self-Tuning Control," *Automatica,* Vol. 20, No. 1, 1984, pp. 15-29.

[21]Toivonen, H., "A Multiobjective Linear Quadratic Gaussian Control Problem," *IEEE Transactions of Automatic Control,* Vol. AC-29, March 1984, pp. 279-280.

[22]Hughes, P.C. and Skelton, R.E., "Controllability and Observability for Flexible Spacecraft," *Journal of Guidance and Control,* Vol. 3, Sept.-Oct. 1980, pp. 452-459.

[23]Hughes, P.C. and Skelton, R.E., "Controllability and Observability of Linear Matrix-Second-Order Systems," *Journal on Applied Mechanics,* Vol. 47, June 1980, pp. 415-420.

[24]Kwakernaak, H. and Sivan, R., *Linear Optimal Control Systems,* John Wiley and Sons, New York, 1972.

[25]VanderVelde, W.E. and Carignan, C.R., "Number and Placement of Control System Components Considering Possible Failures," *Proceedings 1982 American Control Conference,* Arlington, Va., June 1982.

[26]Laskin, R.A., Longman, R.W., and Likins, P.W., "Actuator Placement in Modal Systems Using Bounded-Time Fuel-Optimal Degree of Controllability," *Proceedings, 20th Annual Allerton Conference on Communication Control and Computing,* Oct. 6-8, 1982, pp. 813-822.